Progress In Electromagnetics Research, PIER 42, 261–286, 2003

AN EXACT PERTURBATIVE FORMULATION OF THE DIELECTRIC INTEGRAL EQUATIONS FOR LOSSY INTERFACES

B. A. Davis

ElectroMagnetic Interactions Laboratory
Bradley Department of Electrical and Computer Engineering
Virginia Tech, Blacksburg, VA 24061-0111, USA

R. J. Adams

Department of Electrical and Computer Engineering
University of Kentucky
Lexington, KY 40506-0046, USA

Abstract—In modeling scattering from lossy surfaces, the surface is often approximated as a perfect electric conductor (PEC). However, when loss and wave penetration become important, the IBC model is typically employed and is adequate for many numerical simulations. However, the IBC's range of validity is considered unclear and an accurate quantification of its error is difficult. Consequently, other more exact implementations are necessary, such as integral equation methods. In this paper, a novel numerical implementation of the exact dielectric integral equations has been developed for scattering from a two-dimensional (2D), lossy dielectric interface. The formulation presented herein combines the coupled integral equations to form a single equation. This equation is easily interpreted as the magnetic field integral equation (MFIE) for a 2D, PEC surface with a perturbative term related to the finite conductivity of the surface. The advantage of this perturbation approach is that for ocean and other high loss surfaces, the solution is expected to be rapidly convergent with respect to other approaches and will reproduce the correct result even for surfaces with small curvature radii. Test cases demonstrate increased convergence with increased loss and increased contrast for perpendicular polarization. However with parallel polarization, convergence problems are uncovered and are associated with the Brewster angle effect.

1. INTRODUCTION

In considering scattering from the ocean or terrain, it is common practice to model these surface as perfect electric conductors (PECs). Many numerical techniques have improved the feasibility of simulating low grazing angle incidence. Due to its computational efficiency, a numerical technique of particular interest to the rough surface scattering community is the Method of Multiple Ordered Interactions (MOMI) [1], otherwise known as the Forward-Backward Method [2]. More accurate simulations of natural surfaces, however, require that the effects of the finite conductivity of seawater or the finite conductivity of soil be included in the model. Hence, the incorporation of these characteristics into the simulations are often achieved using an analytical, impedance boundary condition (IBC). With highly conductive seawater, this approximation seems applicable; however, with terrain propagation, the loss tangent of soil at microwave frequencies is significantly smaller than the corresponding loss tangent of seawater, resulting in less accuracy for such surfaces. Additionally, the error introduced by the IBC and its range of validity is unclear when considering low grazing angle (LGA) scattering from surfaces with significant high frequency spectral content. Consequently, one is motivated to find a numerical approach for the dielectric problem that will mimic the convergence properties of an efficient formulation for the PEC surface (e.g., MOMI). Preliminary work on the application of the MOMI to dielectric surfaces has been performed [3, 13]. Unfortunately, the convergence properties were not comparable to the PEC result for

the same geometry since the straight-forward application of MOMI performs an upper/lower triangular factorization on singular operators. In the following, a novel reformulation of the dielectric integral equations is presented as an 'exact' alternative to the IBC formulation of scattering from a two-dimensional, lossy-dielectric interface. This work has been previously introduced by the authors [5, 6].

In the standard dielectric integral equations, a coupled pair are solved [7] or in later works, a single equation is formed [8–10]. The formulation presented herein begins with the coupled integral equations and combines them to form a single equation, each in two-dimensions. Next, this single equation is rearranged so that it reduces to the standard, magnetic field integral equation (MFIE) for a two-dimensional perfect electrically conducting (PEC) surface. For penetrable surfaces, the integral equation derived also contains a perturbation term related to the finite conductivity of the surface. The advantage of this perturbative approach is that for ocean and other high loss or high contrast surfaces, the solution is expected to be rapidly convergent with respect to other exact integral equation approaches.

The new equations are derived for two-dimensional surfaces in both perpendicular (H-pol) and parallel (E-pol) polarizations. Fast convergence is demonstrated for the perpendicular polarization; however, the parallel polarization formulation has revealed some unique qualities of the integral equation itself. In support of these assertions, a short discussion of the properties of the dielectric equations is given. This discussion is followed by preliminary results from a comparison of the Leontovich IBC for scattering from a two-dimensional, lossy-dielectric interface. A complete comparison of the Leontovich IBC and the exact equations will be communicated elsewhere.

2. THE TWO-DIMENSIONAL DIELECTRIC INTEGRAL EQUATIONS

In constructing the integral equation for scattering from a dielectric surface, one begins with coupled integral equations: two each for the lower and the upper media. In the upper medium, the following relationships hold [11].

$$\frac{1}{2}\psi(\boldsymbol{r}) = \psi^{inc}(\boldsymbol{r}) + \int_S \left(\frac{\partial G(\boldsymbol{r},\boldsymbol{r}')}{\partial n'}\psi(\boldsymbol{r}') - \frac{\partial \psi(\boldsymbol{r}')}{\partial n'} G(\boldsymbol{r},\boldsymbol{r}') \right) ds' \qquad (1)$$

The region of integration, S, represents the electromagnetically active surface. Strictly speaking, the integration over S involves an infinite

surface and a "cap" at infinity. The reduction of this infinite problem to the finite surface, S, above can be found in many standard implementations of the MFIE for surface scattering, for example see Kapp and Brown [1] and the references therein. For the Neumann problem, the following integral equation is produced [11],

$$\frac{1}{2}\frac{\partial\psi(\boldsymbol{r})}{\partial n} = \frac{\partial\psi^{inc}(\boldsymbol{r})}{\partial n} + \frac{\partial}{\partial n}\int\limits_S \left(\frac{\partial G(\boldsymbol{r},\boldsymbol{r}')}{\partial n'}\psi(\boldsymbol{r}') - G(\boldsymbol{r},\boldsymbol{r}')\frac{\partial\psi(\boldsymbol{r}')}{\partial n'}\right) ds' \tag{2}$$

The upper medium is characterized by an arbitrary, homogeneous relative permittivity, $\varepsilon_1 = \varepsilon_{r1} - j\varepsilon_{i1}$; for simplicity, free space will be used as the upper medium.

In order to simplify the notation, corresponding operator forms for equations (1) and (2) will be used throughout this paper; these are given in equations (3) and (4). Additionally, the normal derivative of the field has been replaced by the expression $\partial_n\psi$. The operator form for (1) is cast

$$\frac{1}{2}\psi = \psi^{inc} + Q_{DD}\psi - Q_{DN}\partial_n\psi \tag{3}$$

Likewise, the operator expression of (2)

$$\frac{1}{2}\partial_n\psi = \partial_n\psi^{inc} + Q_{ND}\psi - Q_{NN}\partial_n\psi \tag{4}$$

A direct comparison of equations (1) and (3) yield the definitions of operators, Q_{DD} and Q_{DN}; likewise, a comparison of (2) and (4) yield definition of the operators Q_{NN} and Q_{ND}. A discussion of the operators is given in greater detail below.

In describing the lower medium, a similar pair of integral equations is created. For simplicity, these integral equations, (5) and (6) are given in only operator form with the corresponding integral operators implied. The functional form of these operators is the same as previously defined in (3) and (4); however, the sign of each operator has changed since the surface normal is pointing into the upper medium.

$$\frac{1}{2}\psi = -\hat{Q}_{DD}\psi + \hat{Q}_{DN}\partial_n\psi \tag{5}$$

$$\frac{1}{2}\partial_n\psi = -\hat{Q}_{ND}\psi + \hat{Q}_{NN}\partial_n\psi \tag{6}$$

Since the medium constants have changed,the lower medium operators are denoted with a "hat", $\hat{Q}$. The lower medium is also a homogeneous dielectric with a complex, relative permittivity, $\varepsilon_2 = \varepsilon_{r2} - j\varepsilon_{i2}$. Finally,

although it is not a necessary restriction, the incident field is assumed to be present in only the upper medium for simplicity.

Pursuing the properties of these operators yields valuable insight into the behavior of the integral equations. Some useful properties of these operators will now be reviewed for use in later sections. The discussion begins with the two operators, Q_{ND} and Q_{DN}. A straightforward method to isolate the essential properties of these operators is their application to a flat surface. The operator, Q_{DN}, is a smoothing operator representing the mapping of the field's normal derivative, $\partial_n\psi$ into the field itself, ψ through the Green's function. This operation is referred to as a Neumann-to-Dirchlet mapping. In electrical engineering, this transformation represents an impedance (or admittance) mapping.

$$Q_{DN}\partial_n\psi \equiv \int\limits_S G(\boldsymbol{r},\boldsymbol{r}')\frac{\partial\psi(\boldsymbol{r}')}{\partial n}ds' \longrightarrow \psi(\boldsymbol{r}) \tag{7}$$

The dual operator, Q_{ND}, is a hypersingular operator which maps the field, ψ into its partial derivative, $\partial_n\psi$. For a given field, ψ , this operation transforms the field (Dirchlet data) to the normal derivative of the field (Neumann data).

$$Q_{ND}\psi \equiv \frac{\partial}{\partial n}\int\limits_S \frac{\partial G(\boldsymbol{r},\boldsymbol{r}')}{\partial n'}\psi(\boldsymbol{r})ds' \longrightarrow \partial_n\psi(\boldsymbol{r}) \tag{8}$$

It is understood that an appropriate limiting procedure must be used to numerically treat the hypersingular kernel. The mappings between the field and its normal derivative ($\partial_n\psi \leftrightarrow \psi$) reveal an implicit impedance transformation as discussed in [12].

The remaining two operators, Q_{DD} and Q_{NN}, are nonsingular smoothing operators after the observation point is taken to the surface and the singularity has been removed. These operators account for the physical and nonphysical interactions on the surface of the scatterer and are zero for a smooth surface. In the PEC, rough surface scattering literature, these operators are encountered in the MFIE formulations.

$$Q_{DD}\psi = \int\limits_S \frac{\partial G(\boldsymbol{r},\boldsymbol{r}')}{\partial n}\psi ds' \tag{9}$$

$$Q_{NN}\partial_n\psi = \int\limits_S \frac{\partial G(\boldsymbol{r},\boldsymbol{r}')}{\partial n'}\frac{\psi(\boldsymbol{r}')}{\partial n}ds' \tag{10}$$

In the flat surface case, these operators are zero. These operators are discussed in detail in [3].

Beginning with the *infinite planar* scattering geometry, only two of the four operators are required: Q_{ND} and Q_{DN}. Since this special case can be guided by known results, the properties of the two operators, Q_{ND} and Q_{DN}, will become apparent. Given an incident plane wave, $\psi = \exp(-jk_x x + jk_z z)$, the continuous eigenvalue spectrum for the hypersingular operator, Q_{ND}, is found from (4) and is given by $(jk_z/2)$. Consequently, the hypersingular operator accentuates high spatial frequency components. As k_x^2 becomes large, the eigenvalues of the hypersingular operator, Q_{ND}, tend toward zero since $k_z^2 = k^2 - k_x^2$. Likewise, the eigenvalue spectrum of the second operator, Q_{DN} for the planar surface problem is easily determined to be $(-1/j2k_z)$. This operator filters the high spatial frequencies, tending to 'smooth' the result.

Due to the complementary filtering properties of these operators, their combination allows high spatial frequencies to pass without significant attenuation or amplification; thus yielding a mesh stable formulation. The following operator/integral identity quantifies this observation.

$$Q_{ND}Q_{DN} = -\frac{1}{4} \tag{11}$$

This identity provides the basis for an advantageous integral preconditioner: further details are provided by Adams [3].

It is interesting to observe for the grazing mode ($k_z = 0$) that the eigenvalue of Q_{DN} is infinite while the eigenvalue of Q_{ND} is zero. This behavior indicates that for a flat surface, the Neumann problem supports a grazing surface wave while the Dirchlet problem does not. A closer examination of the properties of these operators facilitates the development of a direct, spatial-domain representation of the fields excited at a planar dielectric interface [13].

3. NUMERICAL SOLUTION OF THE DIELECTRIC INTEGRAL EQUATIONS

In this section the two-dimensional dielectric integral equations are cast into a more computationally efficient form. The treatment of the equations follows from the standard field decomposition into perpendicular and parallel polarization. Treating these polarizations separately, the dielectric equations for a surface are recast into a form based on the perturbation of the perfectly conducting surface. Examples and discussion of the properties of these equations are found in the following sections

3.1. Perpendicular Polarization ($\psi \to E$)

Starting with the operator form of the integral equations (3) through (6), in perpendicular polarization one replaces the the field quantity, ψ, by the electric field intensity, E. Next, the field, E, in the lower medium is found in terms of its normal derivative from equation (5). Hence, from equation (5), solving for E,

$$E = 2\left(1 + 2\hat{Q}_{DD}\right)^{-1} \hat{Q}_{DN}\partial_n E \tag{12}$$

Although this expression requires the inversion of an operator with N unknowns (e.g., a moment method matrix of dimension, N), fast solution methods, such a the Method of Ordered Multiple Interactions (MOMI)may be used for accelerating this inverse [1]. However, for large conductivity, the inverse operation in (12) is computed in $O(N)$ operations due to the tightly banded nature of the lossy medium operators; these operators become nearly diagonal.

The boundary condition on the electric field intensity requires that the tangential E-field be continuous across an interface for material with free space permeability ($\mu = \mu_0$). In two dimensions with perpendicular polarization, the electric field is always parallel (tangent) to the surface for all incident angles. Consequently, assuming non-magnetic media, the electric field E in the upper medium is the same as the field E in the lower medium. Substituting this boundary condition into equation (4), an integral equation for perpendicularly polarized field incident on a two-dimensional, randomly rough dielectric surface is constructed:

$$\partial_n E = 2\partial_n E^{inc} - 2Q_{NN}\partial_n E + 4Q_{ND}\left(1 + 2\hat{Q}_{DD}\right)^{-1} \hat{Q}_{DN}\partial_n E \tag{13}$$

The right side of this equation is a superposition of three terms. The combination of the first two terms comprise the familiar result for two-dimensional scattering from a surface which is a perfect electric conductor (PEC). The first of these terms is Kirchhoff term and the second incorporates multiple scattering. The last term of equation (13) expresses the dielectric nature of lower medium through the dielectric medium operators, $\hat{Q}_{DN}$ and $\hat{Q}_{DD}$. Again, these operators are nearly diagonal for high-loss surfaces; they essentially behave as diagonally banded matrices with elements that decay exponentially due to the loss. Hence, as one should expect, this last term will become a small perturbation with respect to the PEC solution as loss is increased.

In the solution of these equations, the perturbative result for the dielectric equation is found by gathering the PEC operators on the left,

leaving the composite operator due to the lossy dielectric unchanged and on the right.

$$(I + 2Q_{NN})\partial_n E = 2\partial_n E^{inc} + 4Q_{ND}\left(1 + 2\hat{Q}_{DD}\right)^{-1}\hat{Q}_{DN}\partial_n E \quad (14)$$

Equation (14) describes the penetrable surface as a perturbative adjustment to the PEC integral equation and can be discretized via the Method of Moments (MoM). Rather than using matrix inversion, however, the solution to this equation may again be obtained using more efficient iterative methods. In this study, the MOMI is used. This technique renormalizes the modified integral equation through the re-summation of the dominant multiple scattering interactions on the rough surface [1]. Consequently, the iterative solution is renormalized using the following decomposition; the notation is consistent with the paper by Kapp and Brown [1]

$$\begin{aligned}\partial_n E = {} & 2(I-U)^{-1}(I-L)^{-1}\partial_n E^{inc} + (I-U)^{-1}(I-L)^{-1}LU\partial_n E \\ & +4(I-U)^{-1}(I-L)^{-1}Q_{ND}\left(1 + 2\hat{Q}_{DD}\right)^{-1}\hat{Q}_{DN}\partial_n E \quad (15)\end{aligned}$$

The matrices L and U represent upper and lower triangular matrices, respectively, found from the upper/lower triangular decomposition of the operator on the left side of equation (14). Although simple Neumann iteration was used, this equation is also amenable to solution with Krylov methods including the conjugate gradient method.

A simple simulation was performed for the new dielectric integral equation given by equation (15). A sinusoidal surface was chosen with the following parameters (normalized to the electromagnetic wavelength λ): the height is 1λ; the period is 30λ; and the total surface length was 52λ. The incident field was chosen to be a perpendicularly polarized Gaussian beam with a half power waist of 15λ, incident to the surface at a 30° angle from the surface normal. Hence, this represents a relatively smooth surface; however, it adequately demonstrates the convergence properties of the new formulation as a function of dielectric constants. The problem was discretized to the scale of the upper medium wavelength. However, integration of the Green's function was performed on a scale proportional to the contrast. Discretizing to the lower medium wavelength would only be necessary if a scatterer below the surface, for example, generated field fluctuations at that scale. Figure 1 demonstrates the convergence of the method for different dielectric contrasts, ε_{r2} and a fixed loss, $\varepsilon_{i2} = 5$. Conversely, Figure 2 demonstrates the convergence of the method for varying amount of loss in the media with a fixed dielectric contrast ($\varepsilon_{r2} = 5$). As a reference, the solution of the PEC problem to a normalized residual error of 10^{-3}

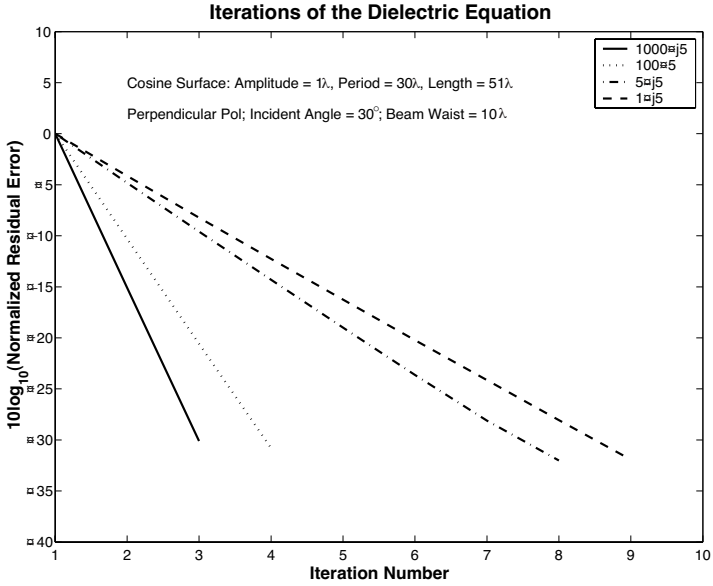

Figure 1. Perpendicular Polarization: Normalized residual error for varying contrast between the media. Convergence of the perturbative dielectric integral equation for a Gaussian beam incident on a cosine surface.

required two iterations. Convergence for the dielectric problem to the same normalized residual error behaved as expected;convergence was more rapid for higher contrasts and greater loss in Figures 1 and 2, respectively.

The number of iterations required to incorporate the effects of the finite loss of the lower medium increases as the loss tangent of the lower medium decreases. This behavior occurs since the numerical IBC is developed as a perturbation of the magnetic field integral equation for PEC surfaces. The various factors affecting the convergence of the modified equation include loss tangent, surface roughness and angle of incidence.

The advantage of the perturbation method with respect to the impedance boundary condition is that it is exact and will reproduce the correct result even for surfaces with significant curvature. The errors in the numerical IBC considered here can be reduced to an arbitrarily small level via iteration of the derived integral equation. One physically important problem where one can expect this to be significant is the problem of grazing backscatter from ocean surfaces.

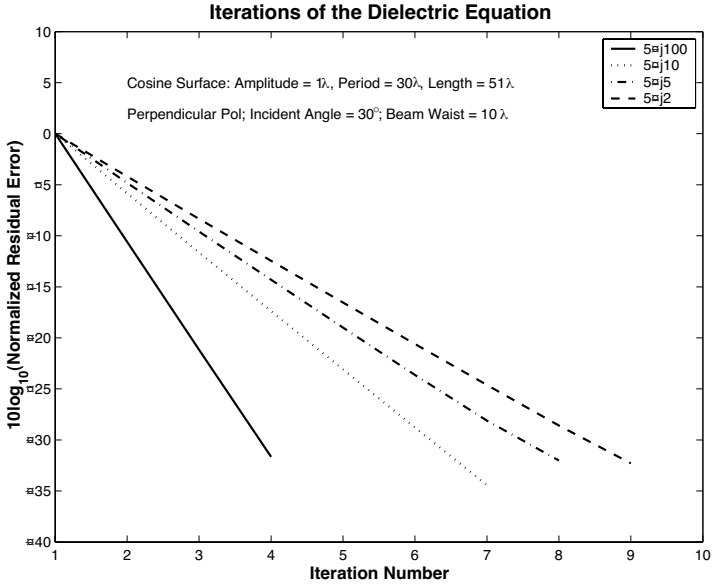

Figure 2. Perpendicular Polarization: Normalized residual error for varying loss in the lower medium. Convergence of the perturbative dielectric integral equation for a Gaussian beam incident on a cosine surface.

For such problems, it is well known that the small wave structure produces the primary contribution to the backscattered field. When these contributions become important, the standard IBC may fail and the present formulation will provide an advantage.

3.2. Comparison of Perpendicular Polarization with the IBC

For comparative purposes, consider the Leontovich Impedance Boundary Condition (LIBC). This model is often implemented for scattering from two-dimensional surface scattering problems due to the simplicity with which it is implemented as well as its typically adequate results. For perpendicular polarization, the LIBC specifies a relationship between the field and it's normal derivative on the surface [14].

$$E = -\frac{j}{k}\sqrt{\frac{\varepsilon_1}{\varepsilon_2}}\frac{\partial E}{\partial n} \tag{16}$$

Surface parameters for the appropriate application of the impedance boundary condition have been outlined by Wang [15]. Assuming

free space in the upper medium, these restrictions are defined with respect to the refractive index in the lower dielectric medium, $\sqrt{\varepsilon_2}$, the smallest radius of curvature, a_{min}, and the free space wavenumber, k_0. Assuming the surrounding medium is free space, the application of the IBC requires a large dielectric contrast

$$|\sqrt{\varepsilon_2}| \gg 1 \tag{17}$$

and a second restricts the surface's curvature

$$|\mathrm{Im}\,\{\sqrt{\varepsilon_2}\}|\, k_0\, a_{min} \gg 1 \tag{18}$$

where $\mathrm{Im}\,\{*\}$ indicates the imaginary part [15]. Substituting equation (16) into equation (4), the following single integral equation is constructed for the dielectric surface excited by a perpendicularly polarized incident field.

$$\partial_n E = 2\partial_n E^{inc} - 2\frac{j}{k_1}\sqrt{\frac{\varepsilon_1}{\varepsilon_2}} Q_{ND}\partial_n E - 2Q_{NN}\partial_n E \tag{19}$$

The use of the IBC has apparently approximated one of the operators found in the exact equation (13) as follows

$$4Q_{ND}\left(1 + 2\hat{Q}_{DD}\right)^{-1}\hat{Q}_{DN} \approx -2\frac{j}{k_1}\sqrt{\frac{\varepsilon_1}{\varepsilon_2}} Q_{ND} \tag{20}$$

The operator $\hat{Q}_{DN}$ has been replaced by term which is an inverse power of the wavenumber, k_2; the implications of this approximation will be examined in the next few paragraphs concerning the flat surface result. Additionally, the operator involving the inverse of $\hat{Q}_{DD}$ has been been completely neglected. Hence, a potentially important multiple scattering term has been discarded. This may be interpreted as a limit on the maximum radius of curvature of the surface and ultimately implies that the IBC can only be exact for a flat surface. The effects of this approximation can be clearly seen by examining scattering from a surface with a small radius of curvature, such as a wedge. These results will be presented in a second paper which focuses directly on the impedance boundary condition.

For illustrative purposes, however, consider the flat surface solution. The flat surface eliminates the impact of one of the approximations of the IBC, ($\hat{Q}_{DD} \approx 0$), since the operators, Q_{NN} and Q_{DD} are zero for a flat surface. Hence, the IBC integral equation (19) reduces to

$$\partial_n E = 2\partial_n E^{inc} - 2Q_{ND}\frac{j}{k_1}\sqrt{\frac{\varepsilon_1}{\varepsilon_2}}\partial_n E \tag{21}$$

When one assumes an incident plane wave, the solution for a single mode can be constructed. Consequently, one may substitute the appropriate eigenvalue for the remaining operator in equation (21). This yields an equation independent of operators since only a single mode is considered.

$$\partial_n E = 2\partial_n E^{inc} + \sqrt{\frac{\varepsilon_1}{\varepsilon_2}} \cos\theta_i \partial_n E \tag{22}$$

Solving for the total field in the upper medium due to the incident plane wave, the integral equation with the IBC approximation yields the solution

$$\partial_n E = \left(\frac{2\sqrt{\varepsilon_2}}{\sqrt{\varepsilon_1}\cos\theta_i + \sqrt{\varepsilon_2}} \right) \partial_n E^{inc} \tag{23}$$

Since the normal derivative of the electric field intensity, $\partial_n E$, is proportional to the surface component of the magnetic field intensity, H, equation (23) may be manipulated to yield a relationship between the incident and the reflected field. Here, the proportionality coefficient is the IBC reflection coefficient for perpendicular polarization

$$\Gamma_{\perp}^{IBC} = \frac{\sqrt{\varepsilon_1}\cos\theta_i - \sqrt{\varepsilon_2}}{\sqrt{\varepsilon_1}\cos\theta_i + \sqrt{\varepsilon_2}} \tag{24}$$

Obviously, if the IBC is exact for the flat surface, this result should match the Fresnel reflection coefficient, found in standard texts [16]. It is note-worthy that if one starts with the exact integral equation (13), assumes a flat surface and examines only one mode, the exact Fresnel coefficients are reproduced as the constant of proportionality between the incident and the reflected field. For a perpendicularly polarized plane wave incident on a flat surface, this reflection coefficient is

$$\Gamma_{\perp} = \frac{\sqrt{\varepsilon_1}\cos\theta_i - \sqrt{\varepsilon_2}\cos\theta_t}{\sqrt{\varepsilon_1}\cos\theta_i + \sqrt{\varepsilon_2}\cos\theta_t} \tag{25}$$

Using the Fresnel coefficient, the total field in the upper medium due to an incident plane wave is

$$\partial_n E = \left(\frac{2\sqrt{\varepsilon_2}\cos\theta_t}{\sqrt{\varepsilon_1}\cos\theta_i + \sqrt{\varepsilon_2}\cos\theta_t} \right) \partial_n E^{inc} \tag{26}$$

A comparison of these expressions for the reflection of a plane wave can be made through equations (24) and (25) or equations (23) and (26). A comparison of the reflection coefficients is given in Figure 3 for a free space upper medium and a dielectric, $\varepsilon = 2 - j1$, in the lower

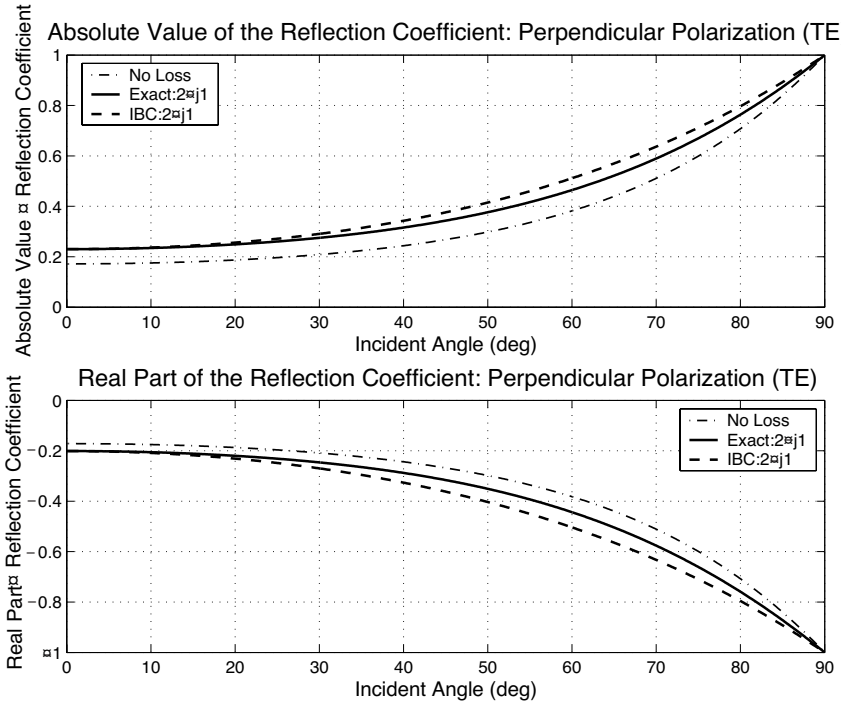

Figure 3. Reflection Coefficients for perpendicular polarization: Fresnel and IBC.

medium. Higher loss and higher contrast result in better agreement between the IBC and the exact result. Examining this figure and the equations, a second limitation of the IBC is now apparent. The IBC will apparently perform well for a transmission angle, θ_t, near 0° and an incident angle, θ_i near 90°; or a dielectric contrast which is large, $(\varepsilon_2 \gg \varepsilon_1)$. Again, these conclusions agree with those given above by Wang [15].

3.3. Parallel Polarization $(\Psi \to H)$

Following a method similar to the previous development, the perturbative integral equation is found by first selecting and solving equation (6) for the field $\partial_n H$ in the lower medium.

$$\partial_n H = -2\left(I - 2\hat{Q}_{NN}\right)^{-1} \hat{Q}_{ND} H \tag{27}$$

Again, the inverse operator in this equation may be efficiently

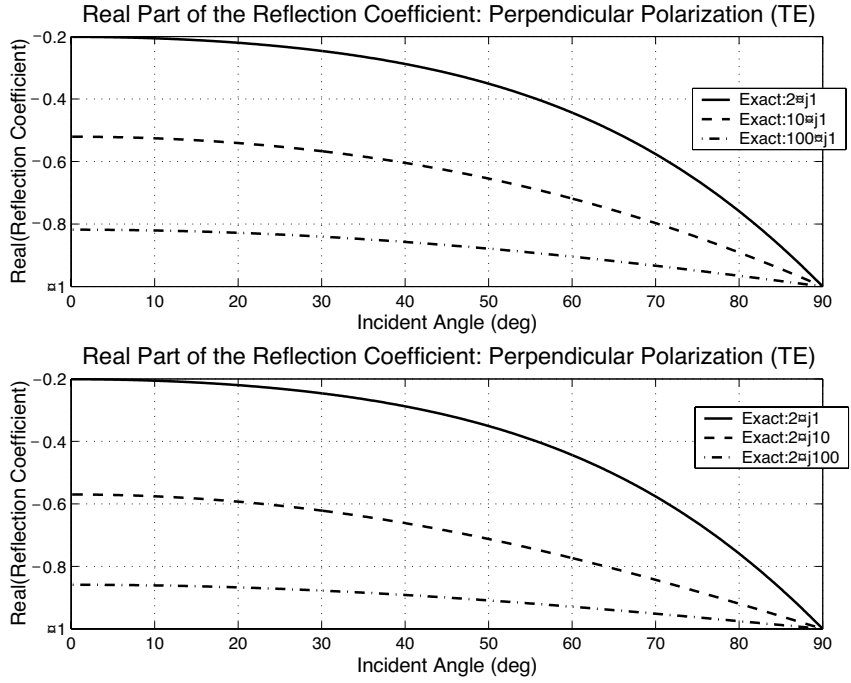

Figure 4. The real part of the re flection coefficient. Higher contrast (or Loss): $\Re e(\Gamma_\perp) \to -1$.

implemented using various techniques such as the MOMI solution. The boundary condition for the normal derivative of the field is then employed. In this case, the boundary condition will impact the final result since a change in permittivity is assumed. This boundary condition relates the normal derivative of the fields.

$$\frac{1}{j\omega\varepsilon_1}\frac{\partial H_1}{\partial n} = \frac{1}{j\omega\varepsilon_2}\frac{\partial H_2}{\partial n} \tag{28}$$

Enforcing this boundary condition, and substituting result into equation (3), the perturbation solution for parallel polarized field incident on a two-dimensional, randomly rough dielectric surface is given.

$$H = 2H^{inc} + 2Q_{DD}H + 4\frac{\varepsilon_1}{\varepsilon_2}Q_{DN}\left(I - 2\hat{Q}_{NN}\right)^{-1}\hat{Q}_{ND}H \tag{29}$$

Again, three terms are present; the first two represent scattering by a perfect electric conductor and the last represents the effect of the

dielectric. This equation can be rearranged into a form dual to the perpendicular result;

$$(I - 2Q_{DD})H = 2H^{inc} + 4\frac{\varepsilon_1}{\varepsilon_2}Q_{DN}\left(I - 2\hat{Q}_{NN}\right)^{-1}\hat{Q}_{ND}H \qquad (30)$$

As in the perpendicular polarization case, this form is amenable to solution by the MOMI technique.

$$\begin{aligned} H = {} & 2(I-U)^{-1}(I-L)^{-1}\partial_n H^{inc} + (I-U)^{-1}(I-L)^{-1}LUH \\ & +4(I-U)^{-1}(I-L)^{-1}\frac{\varepsilon_1}{\varepsilon_2}Q_{ND}\left(1 + 2\hat{Q}_{NN}\right)^{-1}\hat{Q}_{ND}H \end{aligned} \qquad (31)$$

The solution of equation (31) is found using Neumann iteration; the convergence of this iterative approach is illustrated in Figures 5 and 6 for the same sinusoidal surface parameters as used with the perpendicular polarization example of the previous subsection. Obviously, convergence for this polarization presents a problem, since convergence of the Neumann series is only reached for large loss or large dielectric contrast. Low loss and low contrast solutions can actually diverge. This problem is unique to the parallel polarization and is related to the phenomena of the Brewster angle and the behavior of the dielectric integral equations in general. These observations are discussed in Section 3.5.

3.4. Comparison of Parallel Polarization with the IBC

As with the perpendicular case, the Leontovich Impedance Boundary Condition (LIBC) can also be implemented for this problem. Starting with the integral equation (3) describing the field in medium one, and substituting for ψ with the magnetic field intensity, H, one finds

$$H = 2H^{inc} + 2Q_{DD}H - Q_{DN}H \qquad (32)$$

Substituting the LIBC [14]

$$\frac{\partial H}{\partial n} = jk_1\sqrt{\frac{\varepsilon_1}{\varepsilon_2}}H \qquad (33)$$

into (32) yields the following approximate integral equation

$$H = 2H^{inc} + 2Q_{DD}H - 2\left(jk_1\sqrt{\frac{\varepsilon_1}{\varepsilon_2}}\right)Q_{DN}H \qquad (34)$$

The use of the impedance boundary condition has forced the following approximation to the exact operators,

$$4\frac{\varepsilon_1}{\varepsilon_2}Q_{DN}\left(I - 2\hat{Q}_{NN}\right)^{-1}\hat{Q}_{ND} \approx 2\left(jk_1\sqrt{\frac{\varepsilon_1}{\varepsilon_2}}\right)Q_{DN} \qquad (35)$$

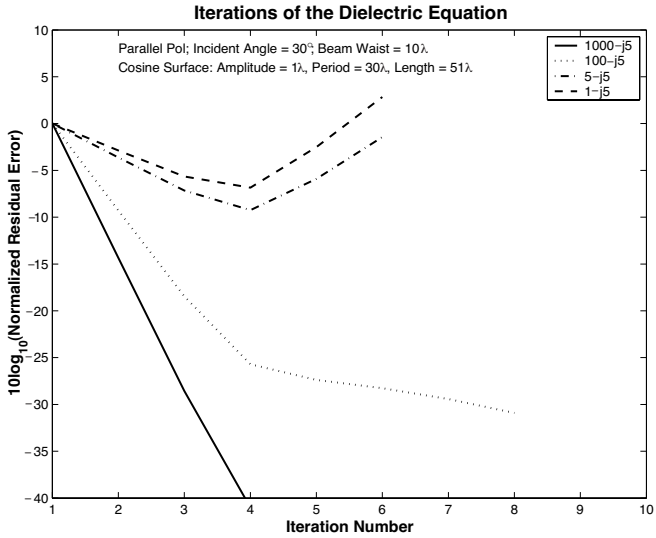

Figure 5. Parallel Polarization: Normalized residual error for varying contrast. Convergence of the perturbative dielectric integral equation for a Gaussian beam incident on a cosine surface.

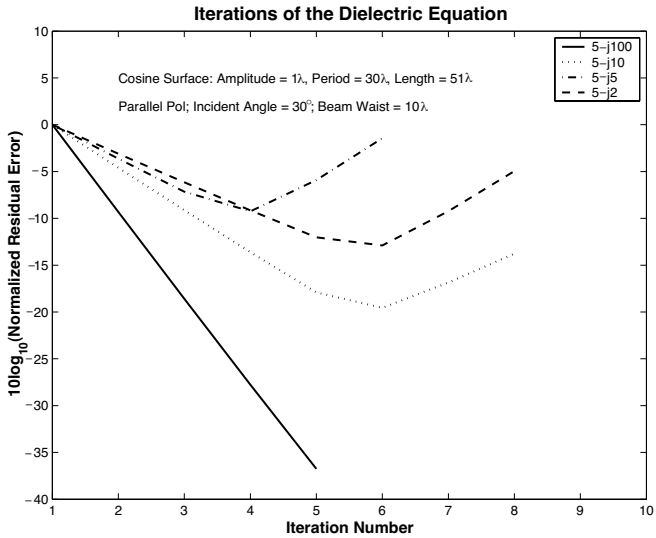

Figure 6. Parallel Polarization: Normalized residual error for varying loss in the lower medium. Convergence of the perturbative dielectric integral equation for a Gaussian beam incident on a cosine surface.

Consequently, one can see that the IBC approximation neglects the multiple scattering term, $\hat{Q}_{NN}$. In addition, this approximation replaces the angle independent form of the integral operator's eigenvalue, $\hat{Q}_{ND} \rightarrow -jk_2/2$ with an approximation, $\hat{Q}_{ND} \rightarrow -jk_2 \cos\theta_t/2$. Hence, this approximation implies a flat surface and an incident plane wave; in other words, the curvature of the surface with respect to the incident field must be large. These results are similar to those found for perpendicular polarization.

As with the previous development, a solution is constructed for an incident plane wave and a flat surface. Since the system is excited by an eigenfunction of the operator, the eigenvalue of the operator is substituted for the operator itself, as follows

$$H = 2H^{inc} - \left(\frac{1}{\cos\theta_i}\right)\frac{\sqrt{\varepsilon_1}}{\sqrt{\varepsilon_2}}H \tag{36}$$

Solving for the total field in the upper medium, the modal solution is formed for an incident plane wave, a flat surface and the implementation of the IBC,

$$H = \left(\frac{2\sqrt{\varepsilon_2}\cos\theta_i}{\sqrt{\varepsilon_1} + \sqrt{\varepsilon_2}\cos\theta_t}\right)H^{inc} \tag{37}$$

This result, in turn, implies a reflection coefficient of the following form

$$\Gamma_{\parallel}^{IBC} = \frac{\sqrt{\varepsilon_1} - \sqrt{\varepsilon_2}\cos\theta_i}{\sqrt{\varepsilon_1} + \sqrt{\varepsilon_2}\cos\theta_i} \tag{38}$$

Using exact plane wave theory, the result for the total field is given by

$$H = \left(\frac{2\sqrt{\varepsilon_2}\cos\theta_i}{\sqrt{\varepsilon_1}\cos\theta_t + \sqrt{\varepsilon_2}\cos\theta_i}\right)H^{inc} \tag{39}$$

and the Fresnel (exact) reflection coefficient is given by,

$$\Gamma_{\parallel} = \frac{\sqrt{\varepsilon_1}\cos\theta_t - \sqrt{\varepsilon_2}\cos\theta_i}{\sqrt{\varepsilon_1}\cos\theta_t + \sqrt{\varepsilon_2}\cos\theta_i} \tag{40}$$

Again one expects for a flat surface, that the IBC will work well as long as the transmission angle, θ_t is near 0°, or the incident angle, θ_i is near 90° or the dielectric contrast is large. Referring to Figure 7, the differences between the reflection coefficient for the IBC and exact theory are displayed for $\varepsilon_2 = 2 - j1$. One notable departure of the exact and the IBC result appears near the Brewster angle.

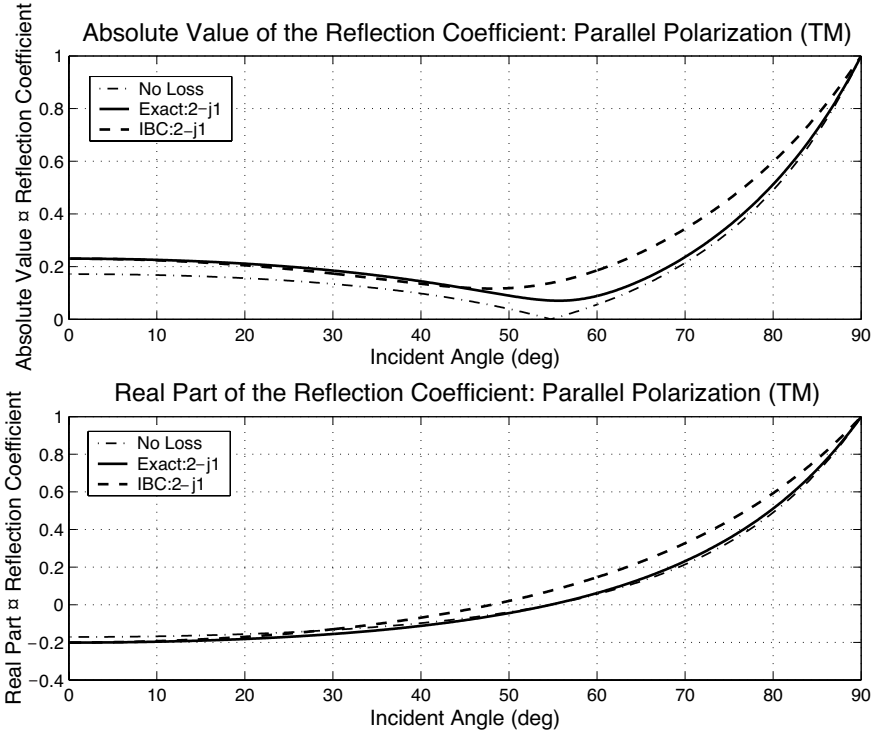

Figure 7. Real part of the reflection coefficients. Higher contrast (or loss): $\Re e(\Gamma_{\|}) \to -1$ near normal incidence; $\Re e(\Gamma_{\|}) \to +1$ near grazing incidence.

3.5. Convergence Properties of the Dielectric Integral Equations

The eigenvalue spectrum of the integral operators for both the perpendicular and the parallel polarizations is constructed in Figure 8; these figures have been created under the assumption of an *infinite half-space of lossless media*. Similarly, Figure 9 displays the eigenvalues of these operators, but with a small loss introduced into the lower medium. In Figure 9, the primary effect of the additional loss was bounding the singularity at the Brewster angle. Although these spectra are not exact for the truncated surfaces used in the simulations found in this work, they provide some insight into the convergence of the solutions. One first considers perpendicular polarization and recalls that the convergence in this case is well-behaved. The eigenvalues for the perpendicular case, bottom of Figures 8 and 9, remain bounded at

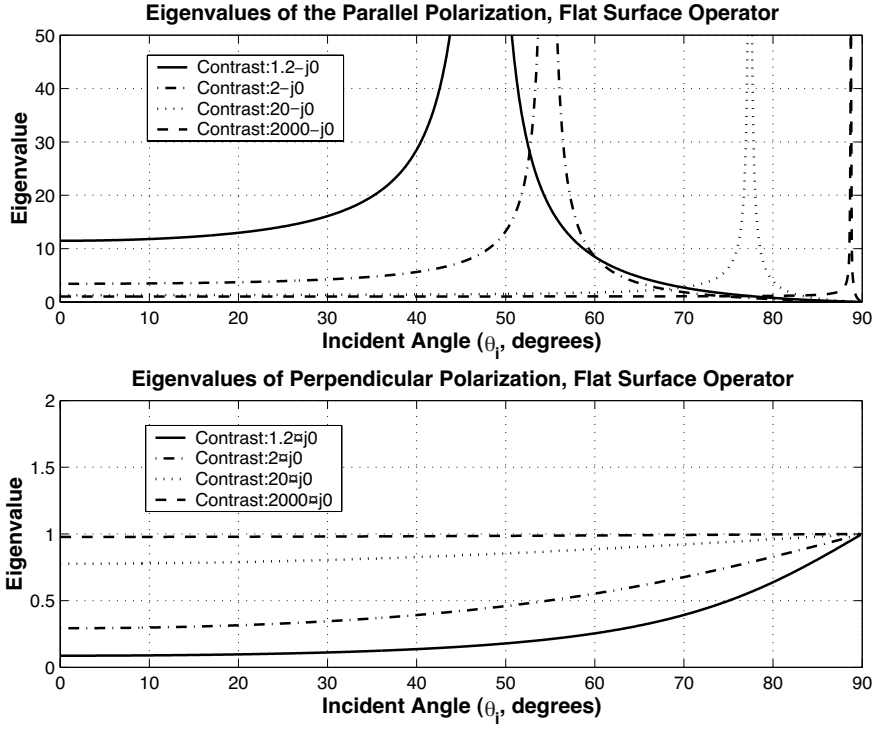

Figure 8. The Eigenvalues of the flat surface operator: Lossless Case; Parallel: $(I - 4\frac{\varepsilon_1}{\varepsilon_2} Q_{DN}\hat{Q}_{ND})$ Perpendicular: $(I - 4Q_{ND}\hat{Q}_{DN})$.

all incident angles. They even approach the ideal value of one for a large dielectric contrast (or larger loss) for all incidence angles. Note that an eigenvalue near one occurs for the perpendicular case since *at grazing incidence, the electric field is consistently parallel to the surface and the PEC boundary condition can be enforced as the loss or contrast approaches infinity* ($E_{\tan}^{total} = 0$). Consequently, one would expect rapid convergence for a perpendicularly polarized incident beam field, since the form of new dielectric integral equation is a perturbation of the PEC equation. In addition, this case should converge more rapidly with larger loss and/or larger dielectric contrast.

On the other hand, examining the parallel polarization case (Figure 8, top), one observes that if the incident angle is near the Brewster angle, the eigenvalue of the parallel operator increases toward infinity. As the contrast approaches infinity, the eigenvalue infinity is pushed out toward grazing incidence. The influence of the Brewster

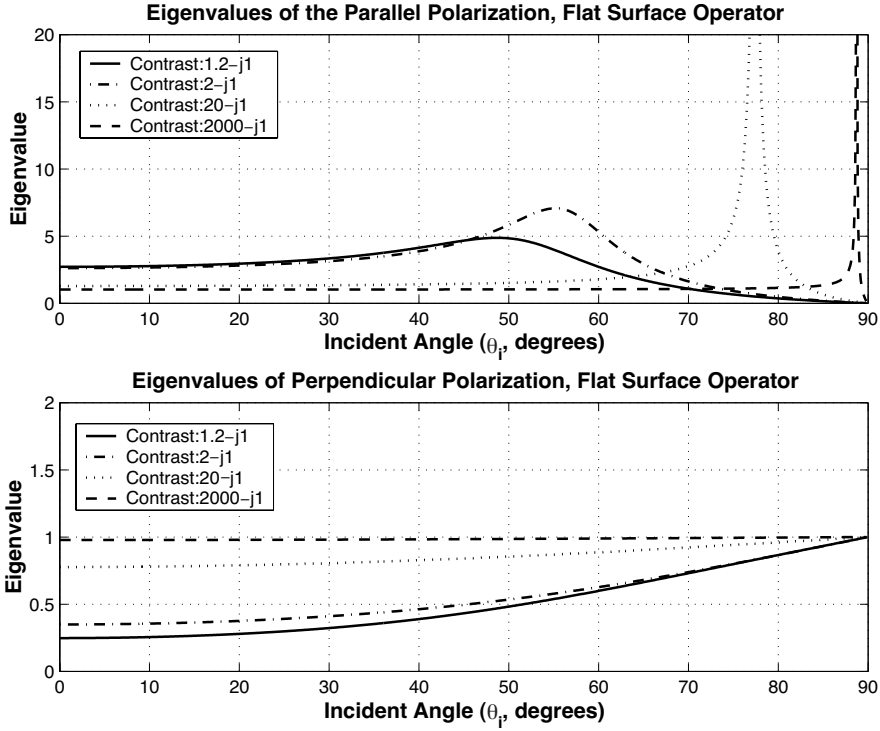

Figure 9. The Eigenvalues of the flat surface operator: Lossy Case; Parallel: $(I - 4\frac{\varepsilon_1}{\varepsilon_2} Q_{DN}\hat{Q}_{ND})$ Perpendicular: $(I - 4Q_{ND}\hat{Q}_{DN})$.

angle effect appears to be greatest with lower contrast interfaces. In the next figure (Figure 9, top), the influence of the loss has suppressed the infinity at the Brewster angle and replaced it with a rounded peak. The introduction of this loss is most noticeable with lower contrasts. On the other hand, one expects that the convergence for an incident, parallel polarized beam may initially converge; however, depending on the error criteria, the parallel case may eventually diverge. Low contrasts or low loss may not converge at all.

Additional insight into the characteristics of the implementation of the integral equations can be found by examining the reflection coefficients. Beginning with perpendicular polarization, an examination of Figure 4 reveals that as the contrast or the loss is increased, the real part of the reflection coefficient approaches negative one, regardless of incidence angle ($\Gamma_\perp \rightarrow -1$). Hence, these integral equations enforce the PEC boundary condition for all real incident angles: the

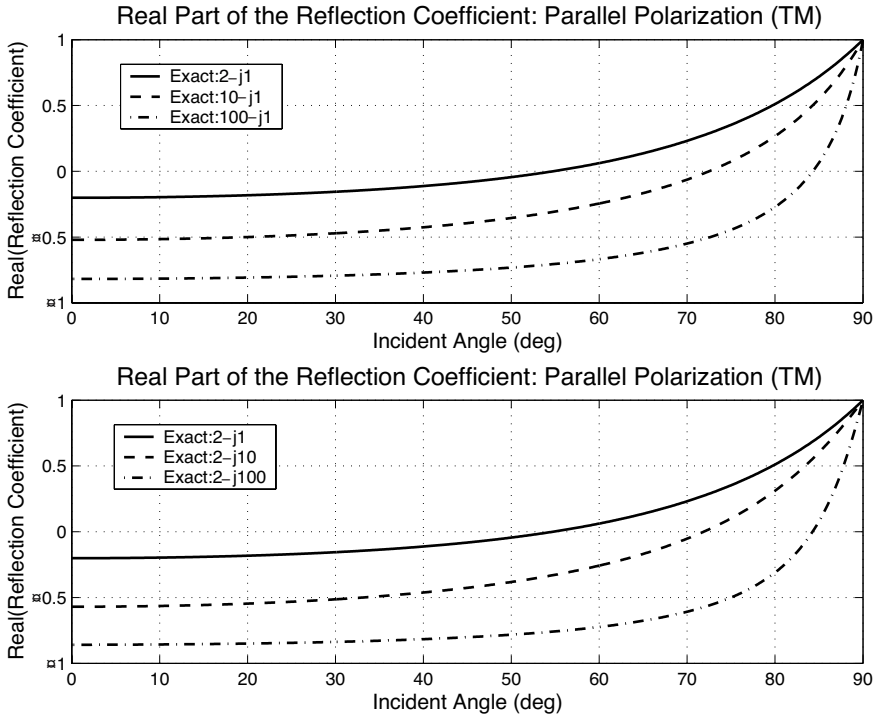

Figure 10. Reflection coefficients for parallel polarization: Fresnel and IBC.

total tangential electric field is zero, a shown below in equation (41).

$$E^{total} = E^{inc} + E^{refl} = (1 + \Gamma_{\perp})E^{inc} = 0 \tag{41}$$

The implications of this observation are more apparent when contrasted with the behavior of parallel polarization.

For parallel polarization, the reflection coefficient is given in Figure 7 and several effects are evident. Near normal incidence, as the loss becomes large, the surface behaves as a PEC surface: the reflected field cancels the incident field which enforces the zero-tangential electric field boundary condition, see equation (42).

$$E^{total} = E^{inc} + E^{refl} = (1 + \Gamma_{\parallel})E^{inc} = 0 \tag{42}$$

However, near grazing incidence, the real part of the reflection coefficient approaches positive one and the electric field is reinforced. The total magnetic field, however, becomes zero; the surface behaves

as if it were a perfect magnetic conductor (PMC) at low grazing angles.

$$H^{total} = H^{inc} + H^{refl} = (1 - \Gamma_{\|})H^{inc} = 0 \tag{43}$$

Figure 10 also shows the reflection coefficient for dielectric coefficients with varying values. Examining this figure, one can see several features. First, the real part of the reflection coefficient is zero at the Brewster angle and has changed sign as the incident angle approaches grazing. Second, unlike the perpendicular case, the real part of the reflection coefficient varies from ($\Gamma_{\|} = -1$ to $\Gamma_{\|} = +1$). Hence, as the contrast or loss is increased, these curves move closer to a reflection coefficient of negative one only near normal incidence. This observation adheres to the form of a second kind integral equation for fields incident near normal. However, since the reflection coefficient for the H-field changes sign after the Brewster angle, the reflected magnetic field intensity will switch from re-enforcing the incident field to cancelling it. The scattering characteristic of the parallel polarization changes from a PEC approximation at normal incidence to a perfect magnetic conductor (PMC) at grazing incidence (total magnetic field becomes zero at the surface). This effect is not encountered with PEC surface simulation since the Brewster angle has been pushed out to 90°.

This instability can be recognized directly from the integral equation itself. Near grazing incidence, the incident field remains $O(1)$ while the field quantity, H approaches $O(\delta)$ or less as the angle approaches grazing; hence, equation (29) for a flat surface becomes

$$H = 2H^{inc} + 4\frac{\varepsilon_1}{\varepsilon_2} Q_{DN}\hat{Q}_{ND}H \tag{44}$$

where H is $O(\delta)$ and H^{inc} is $O(1)$. Therefore, in order to maintain equality, the eigenvalue of the operator must proportionately increase near grazing in order to compensate for the decreasing field magnitude. It can be shown that the eigenvalue of the operator for parallel polarization is in fact proportional to $(\cos\theta^{inc})^{-1}$, when $\theta^{inc} \rightarrow 90°$. Specifically, observe that near grazing, the total magnetic field approaches zero; consequently, the integral equation (29), appears to enforce the perfect magnetic conductor's boundary condition ($H_{\tan}^{total} = 0$).

$$0 = 2H^{inc} + 4\frac{\varepsilon_1}{\varepsilon_2} Q_{DN}\hat{Q}_{ND}H \tag{45}$$

In addition, the unknown only appears under the integral which is reminiscent of the form of a first kind integral equation. The convergence problems inherent in first-kind integral equations have been discussed in [12]. As previously mentioned, the zeroth order

solution has changed from scattering by a PEC surface to scattering by a PMC surface. As a result, the series based on a perturbation of the PEC result is no longer accurate.

4. CONCLUSIONS AND FUTURE EFFORTS

A new, exact approach to the dielectric integral equations in two dimensions has been derived and implemented. This approach provides an alternative to the IBC that does not require the simplifying assumptions of the IBC, yet it is more computationally efficient than standard methods for a class of dielectric surfaces. In the approach proposed here, the solution has been cast as a perturbation to scattering from a PEC surface; the perturbative terms introduce the effects of the finite conductivity of the surface. In addition, through the formulation of the single integral equation, the limitations of the IBC implementation have been verified as operator approximations to the exact integral operators. This investigation into the limitations of the IBC is the subject of an upcoming work. The practical implementation of the new, perturbative dielectric equations also has limitations. For high loss, for example, this formulation behaves very well. It approached the PEC result for higher loss or higher contrast. High loss and high contrast were expected to result in more rapid convergence since the perturbative term diminishes in significance. However, particularly with parallel polarization, the convergence of the Neumann series can be very slow and in some cases, it may diverge. In such cases the proposed equations may still provide a useful preconditioner for a Krylov iterative solver.

The reason for the divergence of the equations has been linked to the Brewster angle effect through an examination of the eigenvalues of the integral operators. Since the operator's eigenvalue blows up in certain spectral regions and remains bounded in others, a spectrally rich incident field will excite these modes. Convergence rate, accordingly, decreases. Since a greater dielectric contrast pushes this critical eigenvalue out toward grazing and decreases the affected spectral region, increasing the dielectric contrast facilitates convergence. Likewise, the addition of loss decreases the peak magnitude of the eigenvalue, thereby decreasing the condition number and increasing convergence rate. An improved method for accommodating the Brewster angle phenomena has been previously introduced and will be addressed in two upcoming papers by the authors in which this effect is specifically treated [13].

Existing dielectric formulations and the new formulation presented herein have undesirable characteristics which lead to numerical insta-

bilities; they are ill-conditioned with respect to mesh discretization. The impedance boundary condition has been introduced into the integral equation for scattering from a dielectric surface and was implemented in this work using the hypersingular operator, Q_{ND} for perpendicular polarization. Without preconditioning, the use of this operator is known to lead to mesh instabilities [12]. Consequently, as the contrast ratio is increased and finer meshes are required, the iterative solution will converge slowly or not at all regardless of the technique used (MOMI, Conjugate Gradient, etc.)

As an alternative to the use of the hypersingular implementation, the electric field boundary condition may be used to construct the integral equation [17]. In the PEC limit ($\varepsilon_i \to j\infty$), however, this formulation reduces to the ill-posed electric field integral equation (EFIE). Numerically this leads to a poorly conditioned matrix for fine discretization. In addition, this formulation is not as useful in the high contrast, no loss limit ($\varepsilon_r \to \infty$). Finally, in an extension of the EFIE approach to three-dimensions, the hypersingular operator cannot be avoided since the EFIE-type kernel is always hypersingular in 3-D. As a consequence, the resulting integral equation is ill-posed, even for high-loss surfaces. This means that, as the discretization interval tends to zero, the number of iterations required to solve it tends to infinity, not to mention that a MOMI-type factorization becomes infeasible.

The poor conditioning of these equations has driven the need for a formulation which asymptotically leads to the correct results. In the PEC implementation of the magnetic Field Integral Equation (MFIE), for example, this asymptotic limit yields the Kirchhoff term. Consequently, a new dielectric formulation which mimics this result of the MFIE is desirable and this approach is the subject of recent works by the authors; an introduction to this work has appeared [13].

ACKNOWLEDGMENT

The authors would like to thank Professor Gary S. Brown, Dr. Jakov Toporkov and Dr. Raid Awadallah for their support and numerous helpful discussions on this subject.

REFERENCES

1. Kapp, D. A. and G. S. Brown, "A new numerical method for rough-surface scattering calculations," *IEEE Transactions on Antennas and Propagation*, Vol. AP-44, No. 5, 711–721, 1996.
2. Holliday, D., L. L. DeRaad Jr., and G. J. St-Cyr, "Forwardbackward: A new method for computing lowgrazing scattering," *IEEE*

Transactions on Antennas and Propagation, Vol. AP-44, No. 5, 722–729, 1996.

3. Adams, R. J., "A class of robust and efficient iterative methods for wave scattering problems," Ph.D. thesis, Virginia Polytechnic Institute and State University, Blacksburg, VA, December 1998.
4. Adams, R. J. and G. S. Brown, "A combined field approach to scattering from infinite elliptical cylinders using the method of ordered multiple interactions," *IEEE Transactions on Antennas and Propagation*, Vol. 47, No. 2, 364–375, 1999.
5. Adams, R. J., B. A. Davis, and G. S. Brown, "The use of a numerical impedance boundary condition with approximate factorization preconditioners for scattering from rough surfaces," *Progress in Electromagnetics Research Symposium*, 421, Boston, MA, July 2000.
6. Davis, B. A., "Propagation and scattering of waves by terrain features," Ph.D. thesis, Virginia Polytechnic Institute and State University, Blacksburg, VA, July 2000.
7. Poggio, A. J. and E. K. Miller, "Integral equation solutions of three dimensional scattering problems," *Computer Techniques in Electromagnetics*, R. Mittra (ed.), Chapter 4, Plenum, New York, NY, 1971.
8. Marx, E., "Alternative single integral equation for scattering by a dielectric," *IEEE Antennas and Propagation Society Symposium Digest*, 906–909, 1992.
9. Kleinman, R. E. and P. A. Martin, "On single integral equations for the transmission problem in acoustics," *SIAM J. Appl. Math.*, Vol. 48, 307–325, 1988.
10. Glisson, A. W., "An integral equation for electromagnetic scattering from homogeneous dielectric bodies," *IEEE Transactions on Antennas and Propagation*, Vol. AP-32, No. 2, 173–175, 1984.
11. Morita, N., N. Kumagai, and J. R. Mautz, *Integral Equation Methods for Electromagnetics*, Artech House, Boston, 1990.
12. Adams, R. J. and G. S. Brown. "Stabilisation procedure for electric field integral equation," *Electronics Letters*, Vol. 35, No. 23, 2015–2016, 1999.
13. Adams, R. J. and B. A. Davis, "Direct spatial-domain representation for the fields excited by an arbitrary incident field at a planar dielectric interface," *IEEE AP-S International Symposium and USNC/URSI National Radio Science Meeting*, 220, Boston, MA, July 2001.
14. Mitzner, K. M., "An integral equation approach to scattering from

a body of finite conductivity," *Radio Science*, Vol. 2, 1459–1470, 1967.

15. Wang, "Limits and validity of the impedance boundary condition on penetrable surfaces," *IEEE Transactions on Antennas and Propagation*, Vol. AP-35, No. 4, 453–457, April 1987.
16. Harrington, R. F., *Time-Harmonic Electromagnetic Fields*, McGraw Hill, New York, 1961.
17. West, J. C., "Low-grazing scattering from breaking water waves using an impedance boundary mm/gtd approach," *IEEE Transactions on Antennas and Propagation*, Vol. 46, No. 1, 93–100, 1998.